

# Impaired intrinsic immunity to HSV-1 in human iPSC-derived TLR3-deficient CNS cells

Fabien G. Lafaille<sup>1,2\*</sup>, Itai M. Pessach<sup>3,4\*</sup>, Shen-Ying Zhang<sup>5,6\*</sup>, Michael J. Ciancanelli<sup>5</sup>, Melina Herman<sup>5,6</sup>, Avinash Abhyankar<sup>5</sup>, Shui-Wang Ying<sup>7</sup>, Sotirios Keros<sup>8</sup>, Peter A. Goldstein<sup>7</sup>, Gustavo Mostoslavsky<sup>9</sup>, Jose Ordovas-Montanes<sup>3</sup>, Emmanuelle Jouanguy<sup>5,6</sup>, Sabine Plancoulaine<sup>6</sup>, Edmund Tu<sup>1,2</sup>, Yechiel Elkabetz<sup>10</sup>, Saleh Al-Muhsen<sup>11</sup>, Marc Tardieu<sup>12</sup>, Thorsten M. Schlaeger<sup>13</sup>, George Q. Daley<sup>13</sup>, Laurent Abel<sup>5,6</sup>, Jean-Laurent Casanova<sup>5,6,14</sup>, Lorenz Studer<sup>1,2</sup> & Luigi D. Notarangelo<sup>3,15</sup>

**In the course of primary infection with herpes simplex virus 1 (HSV-1), children with inborn errors of toll-like receptor 3 (TLR3) immunity are prone to HSV-1 encephalitis (HSE)<sup>1–3</sup>. We tested the hypothesis that the pathogenesis of HSE involves non-haematopoietic CNS-resident cells. We derived induced pluripotent stem cells (iPSCs) from the dermal fibroblasts of TLR3- and UNC-93B-deficient patients and from controls. These iPSCs were differentiated into highly purified populations of neural stem cells (NSCs), neurons, astrocytes and oligodendrocytes. The induction of interferon- $\beta$  (IFN- $\beta$ ) and/or IFN- $\lambda$ 1 in response to stimulation by the dsRNA analogue polyinosinic:polycytidylic acid (poly(I:C)) was dependent on TLR3 and UNC-93B in all cells tested. However, the induction of IFN- $\beta$  and IFN- $\lambda$ 1 in response to HSV-1 infection was impaired selectively in UNC-93B-deficient neurons and oligodendrocytes. These cells were also much more susceptible to HSV-1 infection than control cells, whereas UNC-93B-deficient NSCs and astrocytes were not. TLR3-deficient neurons were also found to be susceptible to HSV-1 infection. The rescue of UNC-93B- and TLR3-deficient cells with the corresponding wild-type allele showed that the genetic defect was the cause of the poly(I:C) and HSV-1 phenotypes. The viral infection phenotype was rescued further by treatment with exogenous IFN- $\alpha$  or IFN- $\beta$  (IFN- $\alpha/\beta$ ) but not IFN- $\lambda$ 1. Thus, impaired TLR3- and UNC-93B-dependent IFN- $\alpha/\beta$  intrinsic immunity to HSV-1 in the CNS, in neurons and oligodendrocytes in particular, may underlie the pathogenesis of HSE in children with TLR3-pathway deficiencies.**

Childhood HSE is a rare, life-threatening, central nervous system (CNS)-restricted complication of primary infection with HSV-1, an almost ubiquitous virus that is typically innocuous<sup>4</sup>. Children with HSE are not unusually susceptible to other infectious agents, including viruses, or even to HSV-1-related diseases affecting sites other than the CNS<sup>4,5</sup>. HSV-1 reaches the CNS from the oral and nasal epithelium, via the cranial nerves<sup>4</sup>. We identified autosomal recessive UNC-93B deficiency as the first genetic aetiology of childhood HSE<sup>1</sup>. UNC-93B is required for TLR3, TLR7, TLR8 and TLR9 responses<sup>1,6</sup>. We then identified autosomal-recessive or autosomal-dominant deficiencies of TLR3 (refs 2 and 3), TRAF3 (ref. 7), TRIF<sup>8</sup> and TBK1 (ref. 9), revealing that childhood HSE can be due to the impairment of TLR3 immunity.

HSV-1 produces double-stranded (dsRNA) during its replication<sup>10,11</sup> and the dsRNA-sensing TLR3 is expressed and functional in non-haematopoietic (neurons, astrocytes, oligodendrocytes) and haematopoietic (microglia) CNS-resident cells, which produce IFN- $\beta$  and IFN- $\lambda$  in response to TLR3 stimulation<sup>12–15</sup> and can be infected with HSV-1 *in vitro*<sup>13,16–19</sup>. We therefore surmised that the pathogenesis of HSE in patients with TLR3-pathway deficiencies may involve impaired TLR3-dependent IFN- $\alpha/\beta$  and/or IFN- $\lambda$  immunity to HSV-1 in the CNS.

We tested this hypothesis by generating induced pluripotent stem cells (iPSCs) from control, UNC-93B- and TLR3-deficient dermal fibroblasts (Supplementary Table 1). We first derived and fully characterized iPSC lines from a healthy child, from an HSE child with autosomal-recessive complete UNC-93B deficiency<sup>1</sup>, and from a patient with autosomal-recessive complete TLR3 deficiency<sup>2</sup>, by reprogramming primary dermal fibroblasts, as described previously<sup>20</sup> (Supplementary Fig. 1 and Methods). A robust stemness and pluripotency profile, karyotypic integrity and patient-specific origin of the iPSCs were confirmed (Supplementary Fig. 1). Whole-exome sequencing for one control, one TLR3-deficient and two UNC-93B-deficient iPSC lines revealed more than 99.9% concordance with the corresponding parental fibroblast lines, in terms of exonic genetic variability (Supplementary Table 2). No synonymous or non-synonymous germline and somatic rare variants of any of the 21 known TLR3-pathway genes were found in parental fibroblast and iPSC lines, respectively (Supplementary Table 3). We also used two additional, previously described healthy control iPSC lines<sup>21,22</sup> for subsequent experiments (Supplementary Table 1).

We next induced the differentiation of iPSCs into all major non-haematopoietic CNS-resident cells, including neural stem cells (NSCs), neurons, oligodendrocytes and astrocytes<sup>23,24</sup>. The selective derivation of each individual neural lineage required a multistep iPSC-differentiation approach combined with fluorescence-activated cell sorting (FACS)-mediated cell purification (Fig. 1a). Neural differentiation of UNC-93B-deficient iPSCs, TLR3-deficient iPSCs, control iPSCs and control human embryonic stem cells (hESCs) (H9 line) was induced by dual SMAD inhibition<sup>21,24</sup> (Fig. 1a and Supplementary Fig. 2a). The resulting polarized columnar neuroepithelial structures expressed PLZF, ZO1 and PAX6, well-known markers of neural rosettes<sup>23</sup>. Mechanically

<sup>1</sup>Center for Stem Cell Biology, Sloan-Kettering Institute for Cancer Research, New York, New York 10065, USA. <sup>2</sup>Developmental Biology Program, Sloan-Kettering Institute for Cancer Research, New York, New York 10065, USA. <sup>3</sup>Division of Immunology, Children's Hospital, Harvard Medical School, Boston, Massachusetts 02115, USA. <sup>4</sup>The Talpiot Medical Leadership Program, Edmond and Lily Safra Children's Hospital, Sheba Medical Center, Tel-Hashomer and the Sackler Faculty of Medicine, Tel Aviv University, Tel Aviv 52621, Israel. <sup>5</sup>St. Giles Laboratory of Human Genetics of Infectious Diseases, The Rockefeller University, New York, New York 10065, USA. <sup>6</sup>Laboratory of Human Genetics of Infectious Diseases, Institut National de la Santé et de la Recherche Médicale, University Paris Descartes, Necker Medical School, U980, Paris 75015, France. <sup>7</sup>C.V. Starr Laboratory for Molecular Neuropharmacology, Department of Anesthesiology, Weill Cornell Medical College, New York, New York 10065, USA. <sup>8</sup>Division of Pediatric Neurology, Department of Pediatrics, Weill Cornell Medical College, New York, New York 10065, USA. <sup>9</sup>Section of Gastroenterology, Department of Medicine and Center for Regenerative Medicine (CRoM), Boston University School of Medicine, Boston, Massachusetts 02118, USA. <sup>10</sup>Laboratory for Pluripotent and Neural Stem Cell Biology, Department of Cell and Developmental Biology, Sackler School of Medicine, Tel Aviv University, Tel Aviv 69978, Israel. <sup>11</sup>Prince Naif Center for Immunology Research, Department of Pediatrics, College of Medicine, King Saud University, Riyadh 11451, Saudi Arabia. <sup>12</sup>Department of Pediatric Neurology, Assistance Publique-Hôpitaux de Paris, Bicêtre Hospital, Kremlin-Bicêtre, 94275, France. <sup>13</sup>Division of Pediatric Hematology/Oncology, Children's Hospital and Dana-Farber Cancer Institute, Boston, Massachusetts 02115, USA. <sup>14</sup>Pediatric Hematology-Immunology Unit, Necker Hospital, Paris 75015, France. <sup>15</sup>The Manton Center for Orphan Disease Research, Children's Hospital, Boston, Massachusetts 02115, USA.

\*These authors contributed equally to this work.

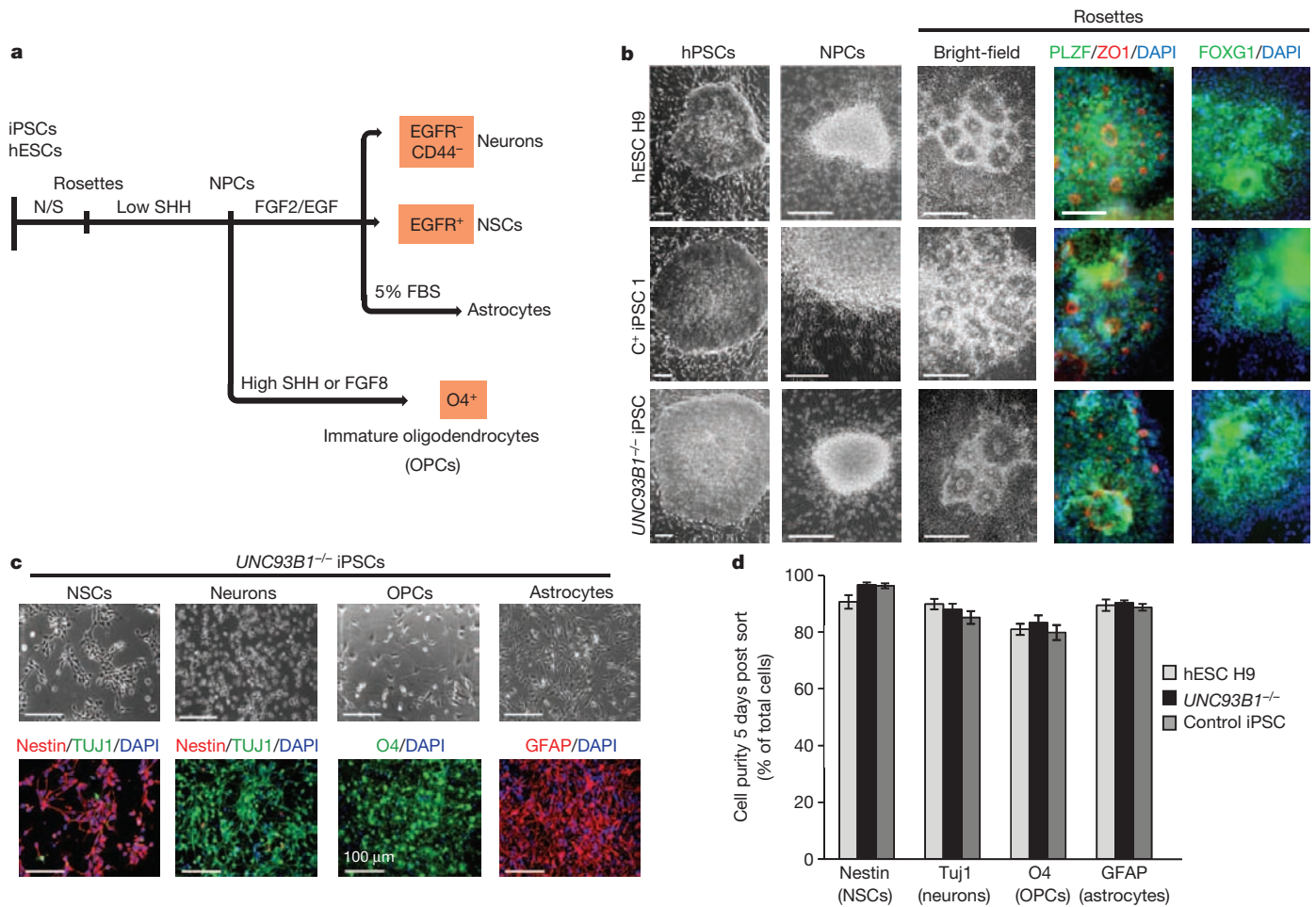


**Figure 1 | Derivation and purification of CNS cells.** **a**, Schematic diagram of the differentiation and purification protocols used. **b**, Representative phase-contrast images showing the morphology of the human pluripotent stem cells (hPSCs), neural rosettes and NPC clusters, from healthy control hESCs, healthy control iPSCs (C<sup>+</sup> iPSC) and *UNC93B1*<sup>-/-</sup> iPSCs. Immunocytochemistry analysis revealed the expression of rosette markers (PLZF and ZO1) and a forebrain marker FOXG1. **c**, Characterization of *UNC93B1*<sup>-/-</sup> iPSC-derived CNS cell types. Upper panels, phase-contrast images showing the characteristic morphology of each type of neural cell; lower panels, immunofluorescence

passed rosettes retained expression of the forebrain marker FOXG1 (Fig. 1b) and yielded neural precursor cells (NPCs) in the presence of FGF2 and EGF (Fig. 1b and Supplementary Fig. 2a). Through differential growth-factor treatment and the use of cell-type-specific surface markers in NPC-stage cells, we were able to isolate highly enriched populations of NSCs, neurons, astrocytes or oligodendrocyte lineage cells (Fig. 1c and Supplementary Fig. 2b, c).

The purified hESC- and iPSC-derived neuronal populations expressed additional lineage-specific markers (Supplementary Fig. 3a) and showed the electrophysiological properties of functional neurons (Supplementary Fig. 3b–e). The identity of the purified glial fibrillary acidic protein (GFAP)-expressing and O4-antigen-expressing glial cell populations was confirmed by global gene expression profiling (Supplementary Fig. 4a, b). Immunocytochemistry for stage-specific markers was used to identify the purified O4 ‘oligodendrocytes’ used throughout this study as a mostly immature (pre-myelinating) oligodendrocyte population (Supplementary Fig. 4c–e, Supplementary Table 4). Quantitative analysis showed that our preparations of NSCs, neurons, astrocytes and oligodendrocytes were highly pure (Fig. 1d), and similar gene-expression profiles were obtained for neurons and astrocytes derived from disease-specific and control cell lines (Supplementary Fig. 5). Our *in vitro* CNS cell-differentiation system

analysis for markers of neural stem cells (nestin), neurons (TUJ1), oligodendrocyte progenitor cells (O4) and astrocytes (GFAP). **d**, Quantification of marker expression for each neural cell type derived from control hESCs, *UNC93B1*<sup>-/-</sup> iPSCs and control iPSCs (error bars, s.e.m.). Scale bars represent 100 μm (b), 50 μm (c; except for O4 staining). High SHH, high concentration of recombinant Sonic hedgehog (C25II (Cys25Ile-Ile)) at 20 ng ml<sup>-1</sup>; low SHH, low concentration of recombinant Sonic hedgehog at 125 ng ml<sup>-1</sup>; N/S, noggin and SB431542 (dual SMAD inhibition).

therefore constitutes a reliable platform for the comparative assessment of CNS cell-specific antiviral immunity.

TLR3 expression has been documented in neurons derived *in vitro* from a human teratocarcinoma cell line<sup>13</sup>, and in primary cells, either in human brain tissues *in situ* (neurons<sup>25</sup>) or isolated from human brain *ex vivo* (oligodendrocytes and astrocytes<sup>12,14,26</sup>), but not in human NSCs (self-renewing, multipotent cells responsible for generating neurons, astrocytes and oligodendrocytes in the CNS)<sup>27</sup>. We detected messenger RNA for key genes of the TLR3-responsive pathway, including *TLR3* and *UNC93B1*, in all four cell types tested (Supplementary Fig. 6a–d), whether differentiated from iPSCs or hESCs. We also detected mRNAs for genes encoding key molecules in the IFN-responsive pathways, including the receptors for IFN- $\alpha/\beta$  and IFN- $\lambda$ , in these cells (Supplementary Fig. 6e–h). Levels of mRNA for the TLR3- and IFN-responsive pathway genes tested were similar, for each CNS cell type, between cells differentiated from control iPSCs, control hESCs and *UNC93B1*-deficient iPSCs, with the expected exception of *UNC93B1*, for which mRNA levels were lower in *UNC93B1*-deficient cells (Fig. 2a and Supplementary Fig. 6a–d).

We then studied TLR3 responses in the same cells. IFN- $\lambda$ 1 and IFN- $\beta$  were induced in a time-dependent manner, by stimulation with the non-specific TLR3 agonist poly(I:C), a dsRNA analogue, in NSCs,

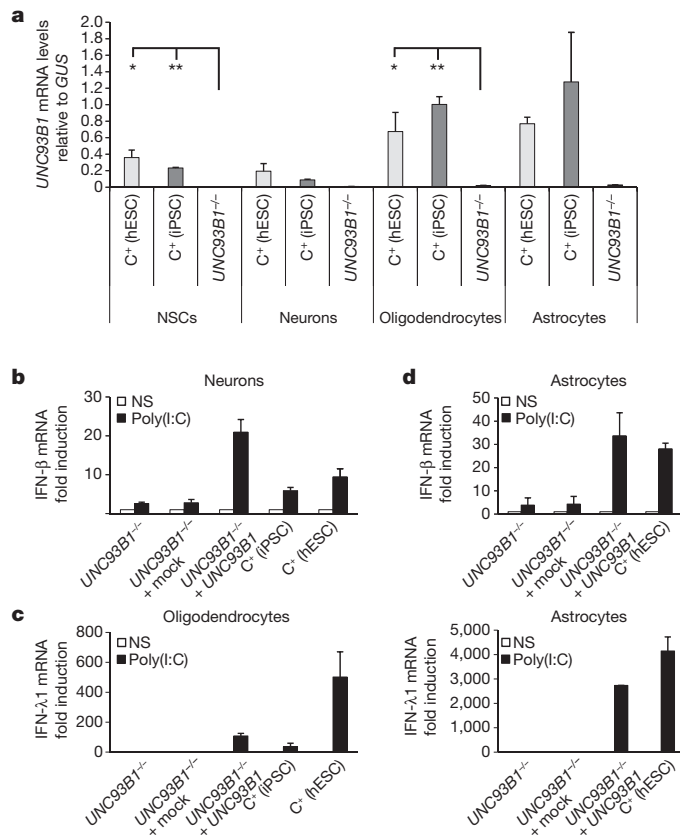


**Figure 2 | UNC-93B-dependent IFN responses to TLR3 in neurons and glial cells.** **a**, *UNC93B1* mRNA levels in CNS cells differentiated from hESCs from a healthy control (C<sup>+</sup> (hESC)) and iPSCs from a healthy control (C<sup>+</sup> (iPSC)), and an UNC-93B-deficient patient (*UNC93B1*<sup>-/-</sup>). NS, not stimulated. **b**, **c**, IFN-β (**b**) or IFN-λ1 (**c**) mRNA induction, after 6 h of poly(I:C) stimulation, in neurons (**b**) or oligodendrocytes (**c**) differentiated from one healthy control hESC line, one healthy control iPSC line, and in *UNC93B1*<sup>-/-</sup> neurons (**b**) or oligodendrocytes (**c**), without lentiviral infection, or after infection with a lentivirus containing human wild-type *UNC93B1* (*UNC93B1*<sup>-/-</sup> + *UNC93B1*) or a mock construct (*UNC93B1*<sup>-/-</sup> + mock). **d**, IFN-β (upper panel) or IFN-λ1 (lower panel) mRNA induction, after 4 h (upper panel) or 6 h (lower panel) of poly(I:C) stimulation, in astrocytes differentiated from hESCs from a healthy control, in *UNC93B1*<sup>-/-</sup> astrocytes, without lentiviral infection, or after infection with a lentivirus containing human wild-type *UNC93B1* (*UNC93B1*<sup>-/-</sup> + *UNC93B1*) or a mock construct (*UNC93B1*<sup>-/-</sup> + mock). Mean values ± s.e.m. were calculated from three (**a**) or two (**b–d**) independent experiments, each carried out in duplicate. Analysis of variance (ANOVA) was carried out for *UNC93B1* mRNA expression levels shown in **a**. When significant, Dunnett's *t*-tests were performed for two-by-two comparisons. \**P* < 0.05, \*\**P* < 0.01 (comparisons between each control line and the patient line, for each cell type).

neurons, oligodendrocytes and astrocytes differentiated from healthy control iPSCs or hESCs, but not in UNC-93B-deficient iPSC-differentiated CNS cells (Fig. 2b–d and Supplementary Fig. 6i–l). The induction of NF-κB1, a key IFN-inducing molecule, and that of MX1, a key IFN-inducible molecule, were both impaired in UNC-93B-deficient oligodendrocytes after poly(I:C) stimulation (Supplementary Fig. 6m, n). The impaired response to poly(I:C) in UNC-93B-deficient CNS cells was consistent with our previous data for UNC-93B-deficient fibroblasts, pointing to a TLR3-dependent response to dsRNA in these cell types<sup>1</sup>. Moreover, impaired poly(I:C) responsiveness in UNC-93B-deficient neurons, oligodendrocytes and astrocytes was rescued by transient expression of the human *UNC93B1* gene (Fig. 2b–d). Thus, the UNC-93B-dependent TLR3 pathway is functional in control human iPSC-derived NSCs, neurons, astrocytes and oligodendrocytes, at least for the induction of antiviral IFN-λ1 and IFN-β in response to poly(I:C).

We thus set out to compare the response to HSV-1 in UNC-93B-deficient and control iPSC or hESC-derived CNS cells after infection with HSV-1 and HSV-1-GFP (green fluorescent protein)<sup>28</sup>. Human NSCs and astrocytes seemed to be more susceptible to HSV-1 infection than neurons and oligodendrocytes, as massive HSV-1-GFP replication was observed earlier (Supplementary Fig. 7 and data not shown). UNC-93B-deficient NSCs and astrocytes derived from two different iPSC lines also showed high levels of HSV-1-GFP replication, similar to those observed in the corresponding cell types derived from two control iPSC lines and the control hESC line (Fig. 3a–c and Supplementary Figs 8a–c and 9a–c). Treatment of UNC-93B-deficient and control NSCs and astrocytes with recombinant IFN-α2B or IFN-β, but not IFN-λ1, decreased HSV-1-GFP replication levels (Supplementary Figs 8a, c–f and 9a, c–g). Moreover, treatment with poly(I:C) decreased HSV-1-GFP replication levels in control, but not in UNC-93B-deficient astrocytes (Supplementary Figs 9f and 10a–d). By contrast, treatment with agonists of TLR9 (CpG-A or CpG-C) did not have such an effect (Supplementary Fig. 10a–d).

When UNC-93B-deficient neurons from the two UNC-93B-deficient iPSC lines were infected with HSV-1-GFP, HSV-1-GFP replication was faster, reaching higher levels than in neurons differentiated from four control iPSC lines or one hESC line (Fig. 3a, d, e and Supplementary Fig. 11a). The treatment of UNC-93B-deficient neurons with IFN-α2B or IFN-β, but not IFN-λ1, rescued this phenotype (Supplementary Fig. 11a). Similar results were obtained with TLR3-deficient neurons that had been differentiated from TLR3-deficient iPSCs<sup>3,20</sup> (Fig. 3e and Supplementary Fig. 11b). The phenotype of enhanced HSV-1 replication in UNC-93B- and TLR3-deficient neurons was rescued by expression of the wild-type human *UNC93B1* and *TLR3* genes, respectively (Fig. 3f and Supplementary Fig. 11b). Finally, higher levels and faster replication of HSV-1-GFP were also observed in UNC-93B-deficient oligodendrocytes than in oligodendrocytes differentiated from control iPSCs or hESCs, and this phenotype was rescued by treatment with IFN-α2B or IFN-β, but not IFN-λ1 (Fig. 3a, g and Supplementary Fig. 11c, d). This is consistent with our previous finding of high susceptibility to HSV-1 and VSV in fibroblasts with TLR3-pathway deficiencies, associated with an impairment of the TLR3-dependent induction of IFN-β and IFN-λ, which can be rescued more effectively by exogenous IFN-α/β than by IFN-λ1 (refs 1–3).

We studied further the production of IFNs and inflammatory cytokines in UNC-93B-deficient and control CNS cells after infection with HSV-1. UNC-93B-deficient neurons, astrocytes and oligodendrocytes produced normal amounts of interleukin-6 (IL-6), as shown by comparison with control iPSC- or hESC-differentiated CNS cell types (Supplementary Fig. 12a–c). UNC-93B-deficient NSCs and astrocytes seemed to produce detectable but lower levels of IFN-λ1 than the control cells tested (Supplementary Fig. 12d, e), suggesting that UNC-93B-independent, TLR3-independent partially compensatory pathways may be involved in triggering IFN responses to HSV-1 in human NSCs and astrocytes. The induction of IFN-β or IFN-λ1 was readily observed in control iPSC- or hESC-differentiated neurons or oligodendrocytes, but was greatly impaired in UNC-93B-deficient neurons and oligodendrocytes, respectively (Supplementary Fig. 12f, g). The induction of MX1 was also impaired in UNC-93B-deficient oligodendrocytes after HSV-1 infection (Supplementary Fig. 12h). Thus, neurons and oligodendrocytes lacking UNC-93B may be highly vulnerable to HSV-1 infection because of an impairment of the cell-autonomous IFN-α/β or IFN-λ immunity.

Our findings suggest that neurons and oligodendrocytes provide strong, intrinsic protective anti-HSV-1 immunity in the CNS, through an intact TLR3 pathway. Although NSCs and astrocytes lacking UNC-93B are not more susceptible to HSV-1 infection than control cells *in vitro*, they may have a role in protective anti-HSV-1 immunity in the CNS *in vivo*. Indeed, mouse astrocytes rely on TLR3 to control HSV-2 (ref. 29). Haematopoietic cell-derived microglial cells, which also



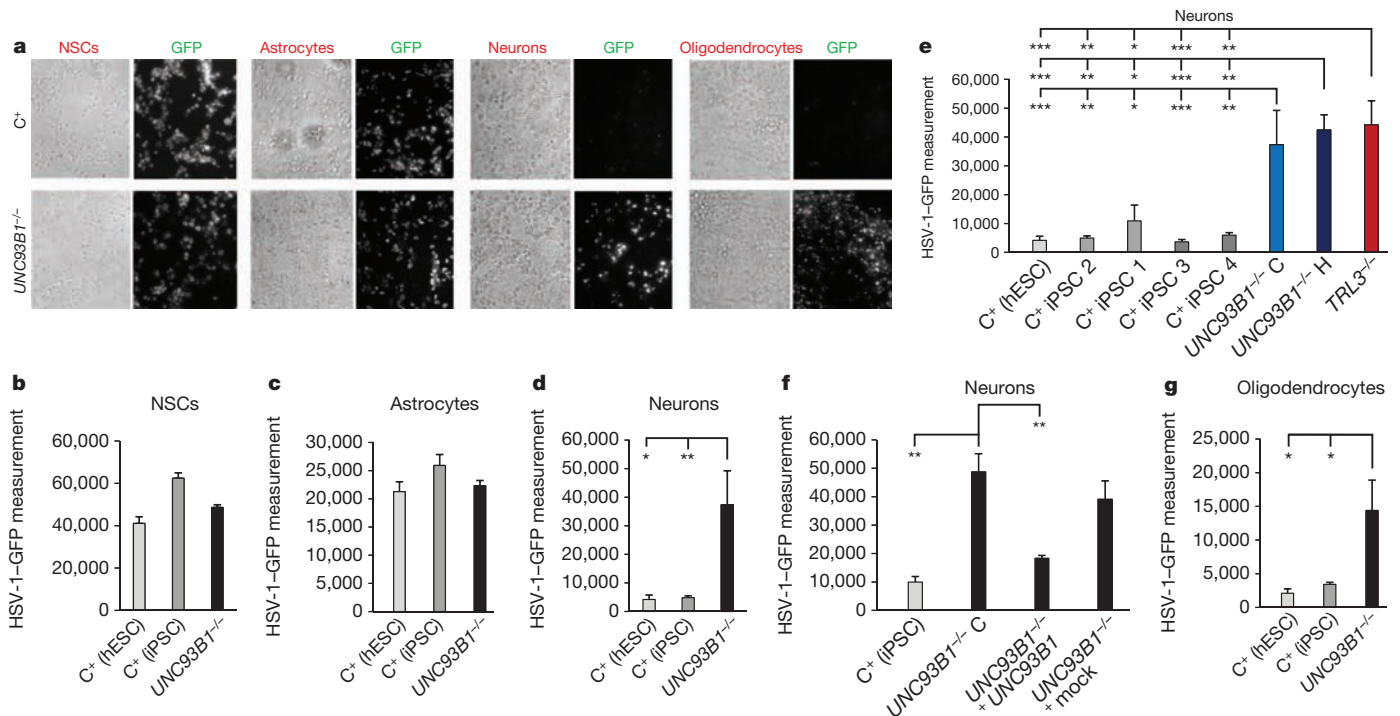


**Figure 3 | High HSV-1 susceptibility in UNC-93B-deficient neurons and oligodendrocytes.** Infection with HSV-1-GFP for 24 h, at a multiplicity of infection of 1, was carried out. **a**, GFP expression in CNS cells differentiated from *UNC93B1*<sup>-/-</sup> iPSCs or from hESCs from a healthy control (C<sup>+</sup>) was visualized using fluorescence microscopy. Phase-contrast photomicrographs from the same view are also shown. **b–d** GFP expression in NSCs (**b**), astrocytes (**c**) and neurons (**d**) differentiated from *UNC93B1*<sup>-/-</sup> iPSCs, from hESCs from a healthy control (C<sup>+</sup> (hESC)) and one to two iPSC lines each from up to three healthy controls (C<sup>+</sup> (iPSC)), was assessed with a fluorescence plate reader. The difference in GFP intensity between HSV-1-GFP-infected cells and uninfected cells is shown. **e**, GFP expression in neurons differentiated from two lines (C and H) of *UNC93B1*<sup>-/-</sup> iPSCs, one line of *TLR3*<sup>-/-</sup> iPSCs, a total of four iPSC lines from three healthy controls, one or two lines from each, or from one C<sup>+</sup> hESCs line.

express TLR3 and can be infected with HSV-1 (refs 12, 14, 17), may also contribute to HSE. CNS-intrinsic mechanisms are thus vital for the control of HSV-1 in the course of primary infection in childhood. These new findings add to our previous results that indicated that most leukocytes and keratinocytes from HSE patients with TLR3-pathway deficiencies respond normally to stimulation with poly(I:C) or HSV-1 (refs 2, 3 and 9), and are consistent with the CNS-restricted pattern of lesions during childhood HSE, with no disseminated disease. Human non-haematopoietic cells may be the key to survival during the course of primary infection, extending the concepts of host defence beyond innate and adaptive haematopoietic immunity, to non-haematopoietic ‘intrinsic’ immunity<sup>30</sup>.

## METHODS SUMMARY

**Human iPSC generation.** Fibroblasts from patients or controls were transduced with the polyclonal stem cell cassette (STEMCCA) lentiviral vector and cultured in DMEM medium supplemented with 10% fetal calf serum (FCS), 2 mM L-glutamine, penicillin (50 U ml<sup>-1</sup>) and streptomycin (50 µg ml<sup>-1</sup>) as described previously<sup>20</sup>. After 72 h, cells were transferred onto irradiated mouse embryonic fibroblasts (iMEFs) and the medium was replaced with hESC medium. iPSC colonies with an ESC-like morphology were mechanically isolated 4 to 5 weeks after infection.

**Neural differentiation.** We adapted previously described protocols for neural differentiation<sup>21,23</sup>. Rosettes were collected on day 8 and cultured further to give clusters of proliferating NPCs. nestin<sup>+</sup>/TUJ1<sup>-</sup> NSCs were maintained in N2 medium supplemented with epidermal growth factor (EGF) (20 ng ml<sup>-1</sup>) and fibroblast growth factor 2 (FGF2) (20 ng ml<sup>-1</sup>) (R&D Systems) and B-27 supplement (1:100, Invitrogen) and sorted for EGF-receptor (EGFR) expression. Nestin<sup>-</sup>/TUJ1<sup>+</sup>

neurons were obtained by eliminating EGFR<sup>+</sup> NSCs and CD44<sup>+</sup> non-neural cells from NPCs. For the generation of astrocytes, NPCs were allowed to proliferate in the presence of EGF and FGF2 for 40 to 60 days and were then cultured in medium containing 5% FBS for an additional 15 to 20 days. Immature oligodendrocytes were obtained from NPCs following treatment with SonicC25II (125 ng ml<sup>-1</sup>), FGF8 (100 ng ml<sup>-1</sup>; R&D Systems), brain-derived neurotrophic factor (BDNF) (20 ng ml<sup>-1</sup>) and ascorbic acid (0.2 mM) for 50 to 70 days and sorted for O4. **TLR3 agonists and viral stimulation.** A synthetic analogue of dsRNA, (polyinosinic:polycytidylic acid (poly(I:C)); Amersham), a TLR3 agonist, was used at a concentration of 25 µg ml<sup>-1</sup>, for 2, 4 or 6 h of stimulation. For HSV-1 infection, we used the KOS-1 strain of HSV-1 and a GFP-expressing HSV-1 (HSV-1-GFP<sup>28</sup>), at various multiplicities of infection (MOIs), to infect CNS cells. The induction of IFN-β, IFN-λ and IFN-responsive genes was assessed in these cells, by quantifying mRNA by quantitative polymerase chain reaction with reverse transcription (RT-qPCR).

**Full Methods** and any associated references are available in the online version of the paper.

Received 25 October 2010; accepted 12 September 2012.

Published online 28 October 2012.

- Casrouge, A. *et al.* Herpes simplex virus encephalitis in human UNC-93B deficiency. *Science* **314**, 308–312 (2006).
- Zhang, S. Y. *et al.* TLR3 deficiency in patients with herpes simplex encephalitis. *Science* **317**, 1522–1527 (2007).
- Guo, Y. *et al.* Herpes simplex virus encephalitis in a patient with complete TLR3 deficiency: TLR3 is otherwise redundant in protective immunity. *J. Exp. Med.* **208**, 2083–2098 (2011).
- Whitley, R. J. Herpes simplex encephalitis: adolescents and adults. *Antiviral Res.* **71**, 141–148 (2006).
- Abel, L. *et al.* Age-dependent Mendelian predisposition to herpes simplex virus type 1 encephalitis in childhood. *J. Pediatr.* **157**, 623–629 (2010).

6. Kim, Y. M., Brinkmann, M. M., Paquet, M. E. & Ploegh, H. L. UNC93B1 delivers nucleotide-sensing toll-like receptors to endolysosomes. *Nature* **452**, 234–238 (2008).
7. Pérez de Diego, R. *et al.* Human TRAF3 adaptor molecule deficiency leads to impaired Toll-like receptor 3 response and susceptibility to herpes simplex encephalitis. *Immunity* **33**, 400–411 (2010).
8. Sancho-Shimizu, V. *et al.* Herpes simplex encephalitis in children with autosomal recessive and dominant TRIF deficiency. *J. Clin. Invest.* **121**, 4889–4902 (2011).
9. Herman, M. *et al.* Heterozygous TBK1 mutations impair TLR3 immunity and underlie herpes simplex encephalitis of childhood. *J. Exp. Med.* **209**, 1567–1582 (2012).
10. Jacquemont, B. & Roizman, B. RNA synthesis in cells infected with herpes simplex virus. X. Properties of viral symmetric transcripts and of double-stranded RNA prepared from them. *J. Virol.* **15**, 707–713 (1975).
11. Weber, F., Wagner, V., Rasmussen, S. B., Hartmann, R. & Paludan, S. R. Double-stranded RNA is produced by positive-strand RNA viruses and DNA viruses but not in detectable amounts by negative-strand RNA viruses. *J. Virol.* **80**, 5059–5064 (2006).
12. Bsibsi, M., Ravid, R., Gveric, D. & van Noort, J. M. Broad expression of Toll-like receptors in the human central nervous system. *J. Neuropathol. Exp. Neurol.* **61**, 1013–1021 (2002).
13. Préhaut, C., Megret, F., Lafage, M. & Lafon, M. Virus infection switches TLR-3-positive human neurons to become strong producers of beta interferon. *J. Virol.* **79**, 12893–12904 (2005).
14. Jack, C. S. *et al.* TLR signaling tailors innate immune responses in human microglia and astrocytes. *J. Immunol.* **175**, 4320–4330 (2005).
15. Zhou, L. *et al.* Activation of Toll-like receptor-3 induces interferon-lambda expression in human neuronal cells. *Neuroscience* **159**, 629–637 (2009).
16. Mitchell, B. M., Bloom, D. C., Cohrs, R. J., Gildea, D. H. & Kennedy, P. G. Herpes simplex virus-1 and varicella-zoster virus latency in ganglia. *J. Neurovirol.* **9**, 194–204 (2003).
17. Lokensgard, J. R. *et al.* Robust expression of TNF-alpha, IL-1beta, RANTES, and IP-10 by human microglial cells during nonproductive infection with herpes simplex virus. *J. Neurovirol.* **7**, 208–219 (2001).
18. Bello-Morales, R., Fedetz, M., Alcina, A., Tabares, E. & Lopez-Guerrero, J. A. High susceptibility of a human oligodendroglial cell line to herpes simplex type 1 infection. *J. Neurovirol.* **11**, 190–198 (2005).
19. Marques, C. P., Hu, S., Sheng, W. & Lokensgard, J. R. Microglial cells initiate vigorous yet non-protective immune responses during HSV-1 brain infection. *Virus Res.* **121**, 1–10 (2006).
20. Pessach, I. M. *et al.* Induced pluripotent stem cells: a novel frontier in the study of human primary immunodeficiencies. *J. Allergy Clin. Immunol.* **127**, 1400–1407 (2011).
21. Chambers, S. M. *et al.* Highly efficient neural conversion of human ES and iPS cells by dual inhibition of SMAD signaling. *Nature Biotechnol.* **27**, 275–280 (2009).
22. Kriks, S. *et al.* Dopamine neurons derived from human ES cells efficiently engraft in animal models of Parkinson's disease. *Nature* **480**, 547–551 (2011).
23. Elkabetz, Y. *et al.* Human ES cell-derived neural rosettes reveal a functionally distinct early neural stem cell stage. *Genes Dev.* **22**, 152–165 (2008).
24. Tabar, V. *et al.* Migration and differentiation of neural precursors derived from human embryonic stem cells in the rat brain. *Nature Biotechnol.* **23**, 601–606 (2005).
25. Jackson, A. C., Rossiter, J. P. & Lafon, M. Expression of Toll-like receptor 3 in the human cerebellar cortex in rabies, herpes simplex encephalitis, and other neurological diseases. *J. Neurovirol.* **12**, 229–234 (2006).
26. Farina, C. *et al.* Preferential expression and function of Toll-like receptor 3 in human astrocytes. *J. Neuroimmunol.* **159**, 12–19 (2005).
27. Taupin, P. & Gage, F. H. Adult neurogenesis and neural stem cells of the central nervous system in mammals. *J. Neurosci. Res.* **69**, 745–749 (2002).
28. Desai, P. & Person, S. Incorporation of the green fluorescent protein into the herpes simplex virus type 1 capsid. *J. Virol.* **72**, 7563–7568 (1998).
29. Reinert, L. S. *et al.* TLR3 deficiency renders astrocytes permissive to herpes simplex virus infection and facilitates establishment of CNS infection in mice. *J. Clin. Invest.* **122**, 1368–1376 (2012).
30. Bieniasz, P. D. Intrinsic immunity: a front-line defense against viral attack. *Nature Immunol.* **5**, 1109–1115 (2004).

**Supplementary Information** is available in the online version of the paper.

**Acknowledgements** We thank our patients, their families and physicians; and the members of the three laboratories for helpful discussions and critical reading of this manuscript. The work was funded by grant number 8UL1TR000043 from the National Center for Translational Sciences (NCATS), the National Institutes of Health (NIH), the Rockefeller University, the St. Giles Foundation, the ANR, INSERM, Paris Descartes University, the March of Dimes, NIH grant 5R01NS072381-02 (to J.-L.C., L.S. and L.D.N.), NIH grant 1R03AI0883502-01 (to L.D.N.), NIH grant 1R01NS066390 and the Manton Foundation, the Israeli Centers of Research Excellence (I-CORE), and Gene Regulation in Complex Human Disease, Center No 41/11 (to I.M.P.). F.G.L. is supported by the New York Stem Cell Foundation.

**Author Contributions** F.G.L., I.M.P., S.-Y.Z., J.-L.C., L.S. and L.D.N. designed the experiments. F.G.L., I.M.P., S.-Y.Z., M.J.C., M.H., A. A., G.M., S.-W.Y., S.K., P.A.G., J.O.-M., E.J., E.T., Y.E. and T.M.S. carried out the experiments. S.A. and M.T. helped to obtain materials from patients and interpret the findings. G.Q.D. and L.A. helped to analyse and describe the data. S.-Y.Z. and J.-L.C. wrote the manuscript with the aid of F.G.L., I.M.P., L.S. and L.D.N. F.G.L., I.M.P. and S.-Y. Zhang are equal first authors. J.L.C., L.S. and L.D.N. are co-senior authors.

**Author Information** The transcriptome data have been deposited in the Gene Expression Omnibus database under accession number GSE40593. Reprints and permissions information is available at [www.nature.com/reprints](http://www.nature.com/reprints). The authors declare no competing financial interests. Readers are welcome to comment on the online version of the paper. Correspondence and requests for materials should be addressed to S.-Y.Z. ([shzh289@rockefeller.edu](mailto:shzh289@rockefeller.edu)) or J.L.C. ([jean-laurent.casanova@rockefeller.edu](mailto:jean-laurent.casanova@rockefeller.edu)).

## METHODS

**Cell culture.** Fibroblasts obtained from an UNC-93B-deficient patient, a TLR3-deficient patient and a healthy control were maintained in DMEM medium supplemented with 10% fetal calf serum (FCS), 2 mM L-glutamine, penicillin (50 U ml<sup>-1</sup>) and streptomycin (50 µg ml<sup>-1</sup>). The patients resided in France, where they were followed up and where informed consent was obtained, in accordance with local regulations, with institutional review board (IRB) approval. The experiments described here were conducted in the United States, in accordance with local regulations and with the approval of the IRB of the Rockefeller University, the Harvard Medical School and the Sloan-Kettering Institute for Cancer Research. Induced pluripotent stem cells (iPSCs) and human embryonic stem cells (hESCs; line H9 (WA-09, XX, P40–55) were maintained on CF1-irradiated MEFs (iMEFs, Globalstem) in hESC medium consisting of DMEM with Ham's F12 (Invitrogen) supplemented with 20% Knockout Serum (KOSR, Invitrogen), 10 ng ml<sup>-1</sup> basic fibroblast growth factor (bFGF, Gemini Bio-Products), 1 mM L-glutamine (Invitrogen), 100 µM non-essential amino acids, 100 µM 2-β-mercaptoethanol (Sigma-Aldrich), penicillin (50 U ml<sup>-1</sup>) and streptomycin (50 µg ml<sup>-1</sup>). iPSCs were stimulated to differentiate into embryoid bodies by culture in bFGF-free hESC medium, without co-culture with feeder cells, on non-adherent Petri dishes, as described previously<sup>31</sup>.

**Neural induction and neural subtype specification.** MS5 stromal cells were grown in MEM medium supplemented with 10% FBS and 2 mM L-glutamine<sup>32</sup>. The neural differentiation of hESCs and iPSCs was induced as described previously<sup>33</sup>, but in the presence of Noggin (R&D Systems) and SB431542 (Stemgent) from days 3 to 10 of differentiation (dual-SMAD inhibition<sup>21</sup>), to increase the efficiency of rosette formation. Rosettes were collected mechanically, starting at day 8 of differentiation, and were re-plated under feeder-free conditions on dishes coated with 10 µg ml<sup>-1</sup> polyornithine (Sigma), 2 µg ml<sup>-1</sup> laminin (Cultrex) and 1 µg ml<sup>-1</sup> fibronectin (Fisher), in N2 medium supplemented with Sonic C25 II (20 mg ml<sup>-1</sup>; R&D Systems), ascorbic acid (0.2 mM; Sigma) and BDNF (20 ng ml<sup>-1</sup>; R&D Systems). Rosettes were allowed to proliferate for a further 5 days and were then re-plated, dissociated in Ca<sup>2+</sup>- and Mg<sup>2+</sup>-free Hank's balanced salt solution (HBSS) and re-plated again. Emerging clusters of NPCs were collected for further proliferation or neural subtype specification. For the generation of neural stem cells and neurons, NPCs were maintained in N2 medium supplemented with EGF (20 ng ml<sup>-1</sup>) and FGF2 (20 ng ml<sup>-1</sup>; R&D Systems) and B-27 supplement without vitamin A (1:100; Invitrogen). For the generation of astrocytes, NPCs were allowed to proliferate and were passaged in the presence of EGF and FGF2 for 40 to 60 days and then exposed to N2 medium containing 5% FBS for an additional 15 to 20 days. For the generation of oligodendrocytes, emerging clusters of NPCs were cultured in N2 medium supplemented with Sonic C25II (125 ng ml<sup>-1</sup>), FGF8 (100 ng ml<sup>-1</sup>; R&D Systems), BDNF (20 ng ml<sup>-1</sup>) and ascorbic acid (0.2 mM) for 50 to 70 days.

**Plasmids and vectors.** The polycistronic lentiviral pHAGE-STEMCCA-LoxP vector, carrying the *OCT4*, *SOX2*, *KLF4* and *C-MYC* reprogramming factor genes, has been described elsewhere<sup>34</sup>. Human *UNC93B1* complementary DNA was amplified from existing cDNA sequences with the following primers: forward 5'-ATAATATGGCCACACATATGGAGCGGAGCCG-3' and reverse 5'-GTTGATTAGGATCTACTGTCCTCCTCCGG-3'. The amplified product was inserted downstream from the internal ribosome entry site (IRES) in a pHAGE2-EF1a-DsRedExpress-IRES-W lentiviral vector (available from the Mostoslavsky laboratory), with the In-Fusion Advantage PCR cloning Kit (Clontech).

**Lentivirus production.** Lentiviruses containing STEMCCA or pHAGE2-EF1a-DsRedExpress-IRES-UNC93B1 were produced with a five-plasmid transfection system, in 293T packaging cells, by a slightly modified version of a method described previously<sup>35</sup>. In brief, 293T cells were transfected with STEMCCA or pHAGE2-EF1a-DsRedExpress-IRES-UNC93B1 and four plasmids encoding the packaging proteins Gag-Pol, Rev, Tat and the G protein of the vesicular stomatitis virus (VSV-G), in the presence of the *Trans-IT* 293 transfection reagent (Mirus). Viral supernatants were collected every 12 h, on 2 consecutive days, starting 48 h after transfection, and viral particles were concentrated by ultracentrifugation at 49,000g for 1.5 h at 4 °C.

**Lentiviral infection and human iPSC generation.** We infected 10<sup>5</sup> fibroblasts derived from patients or controls with the concentrated polycistronic STEMCCA lentiviral vector and then cultured them at 37 °C, under an atmosphere containing 5% CO<sub>2</sub>, in 2 ml of hFib medium supplemented with 5 µg ml<sup>-1</sup> protamine sulphate, for 24 h. One day after infection, the viral supernatant was removed and the cells were cultured for 72 h in hFib medium. They were then transferred onto iMEFs and the medium was replaced with hESC medium. iPSC colonies with an ESC-like morphology were mechanically isolated 4 to 5 weeks after infection.

**Immunostaining.** Cells were fixed by incubation in 4% paraformaldehyde for 30 min and permeabilized by incubation with 0.2% Triton X-100 for 30 min. Cells

were stained in blocking buffer (3% BSA; 5% goat serum) with primary (or conjugated) antibodies at 4 °C overnight, washed and stained with secondary antibodies and 1 µg ml<sup>-1</sup> Hoechst 33342 in blocking buffer for 3 h at 4 °C, in the dark. Primary OCT4 and NANOG antibodies (Abcam) were used at a concentration of 0.5 µg ml<sup>-1</sup>, and an Alexa Fluor 555-conjugated anti-rabbit IgG 555 (Invitrogen) was used as the secondary antibody (1:2000). The following conjugated antibodies—TRA-1-60-Alexa Fluor 647, TRA-1-81-Alexa Fluor 488, SSEA-4-Alexa Fluor 647, and SSEA-3-Alexa 488 (Millipore)—were used at a dilution of 1:100. FoxG1 antibody was a gift from S. A. Anderson. Nestin antibody was obtained from Neuromics, TUJ1 antibody from Covance, O4 from Millipore, GFAP from Dako, PLZF from Calbiochem, and ZO1 from Zymed. Images were acquired with a Pathway 435 bioimager equipped with a ×10 objective (BD Biosciences).

**Whole-exome sequencing and analysis.** DNA (3 µg) was extracted from cells and sheared with a Covaris S2 Ultrasonicator (Covaris). An adaptor-ligated library was prepared with the TruSeq DNA Sample Prep Kit (Illumina). Exome capture was carried out with the SureSelect Human All Exon 50 Mb kit (Agilent Technologies). Paired-end sequencing was performed on an Illumina HiSeq 2000 (Illumina), generating 100-base reads. The sequences were aligned with the human genome reference sequence (hg19 build) using the BWA aligner<sup>36</sup>. Downstream processing was carried out with the Genome Analysis Toolkit (GATK)<sup>37</sup>, SAM tools<sup>38</sup> and Picard Tools (<http://picard.sourceforge.net>). Variant calls were made with GATK UnifiedGenotyper. All calls with a Phred-scaled SNP quality of ≤20 were filtered out. GATK VariantEval was used to compare the call sets for fibroblasts and iPSCs.

**FACS-mediated cell purification.** Cells were dissociated with Accutase (Innovative Cell Technologies) and subjected to FACS with O4 (1:300; Millipore), CD44 FITC (2 µl per 10<sup>6</sup> cells; Abcam), and EGFR PE (10 µl per 10<sup>6</sup> cells; Abcam) antibodies, on a FACS Aria II machine (BD).

**Karyotype analysis.** Karyotyping and G-banding were carried out blind, by Cell Line Genetics.

**Mutation analysis.** Whole-genome DNA was isolated from fibroblasts and iPSCs with the QiAMP DNA Kit (Qiagen). Exon 8 of the *UNC93B1* gene was amplified with the forward primer GCGTGGCTTTGTGCTGAGAG and the reverse primer CAGGAGGGGATATTTGGGA. Reaction products were purified with the QIAquick PCR purification kit (Qiagen) and sequenced by the DF/HCC DNA Sequencing Facility. The results were analysed with Sequencher 4.8 software (Gene Codes Corporation).

**Microarray analysis.** Total RNA was extracted with Trizol reagent (Invitrogen). RNA was collected from astrocytes and from CD44<sup>-</sup>/EGFR<sup>+</sup> neurons differentiated from control hESCs or UNC-93B-deficient iPSCs. The RNA was then processed by the MSKCC Genomic core facility and hybridized with Illumina human HT-12 oligonucleotide arrays. Gene-expression analysis was carried out with the Partek Genomics Suite: following quantile normalization, all the genes displaying differential expression (FDR of 0.05, fold change of at least ±2) with respect to hESC (total of 7,210 genes) in each population were visualized by clustering. Raw data for the microarray analyses performed in this study are available from the public repository of GEO Data Sets (accession number GSE40593).

**Electrophysiology.** Whole-cell current clamp recordings were performed at room temperature (23–24 °C) in a Multiclamp 700B amplifier (Molecular Devices), as described previously<sup>39,40</sup>. Neurons were identified under a Nikon microscope equipped with a ×4 objective and a ×40 water-immersion objective. Cells were continuously perfused with freshly prepared extracellular solution containing 126 mM NaCl, 26 mM NaHCO<sub>3</sub>, 3.6 mM KCl, 1.2 mM NaH<sub>2</sub>PO<sub>4</sub>, 1.2 mM MgCl<sub>2</sub>, 2 mM CaCl<sub>2</sub> and 17 mM glucose, and the solution was saturated with 95% O<sub>2</sub> and 5% CO<sub>2</sub>. The intracellular solution contained 135 mM potassium gluconate, 5 mM NaCl, 10 mM HEPES, 0.5 mM EGTA, 3 mM potassium ATP, 0.2 mM sodium guanosine triphosphate (GTP) and 10 mM sodium phosphocreatine. The pH was adjusted to 7.3 with KOH, and the osmolarity of the solution was approximately 290 milliosmoles (mOsm). Input resistance was calculated from the voltage response elicited by the intracellular injection of a depolarizing (+10- or +20-pA) current pulse. Current steps were applied for 1 s to evoke action potentials. Liquid junction potentials were calculated and corrected off-line. Data were analysed with Clampfit (Molecular Devices) and SigmaPlot 11 (Systat Software) and are presented as means ± s.e.m.

**Quantitative PCR with reverse transcription.** For analysis of the expression profiles of key genes involved in stem cell properties and pluripotency, total RNA was extracted with the mirVana RNA isolation kit (Ambion). We reverse-transcribed 100 ng of total RNA to generate cDNA, in qScript cDNA Supermix (Quanta). RT-qPCR was then performed in an AB 7500 Real-Time PCR system (Applied Biosystems), with the PowerSYBR Green PCR Master Mix (Applied Biosystems). The results were analysed with SDSv1 Software and normalized with respect to β-actin gene expression. Expression levels were determined by relative



quantification using the comparative Ct (ddC<sub>T</sub>) method and are expressed relative to those in the individual parental cell lines. The primer sequences used have been described elsewhere<sup>41</sup>. We assessed the expression levels of genes of the TLR3 and IFN pathways and of the genes for IFN- $\beta$ , IFN- $\lambda$ , NF- $\kappa$ B and MX1, by extracting total RNA from NSCs, neurons, oligodendrocytes and astrocytes. RNA was reverse-transcribed directly, with oligo(dT), to determine mRNA levels for TLR3- and IFN-pathway genes and for IFN- $\beta$ , IFN- $\lambda$ , NF- $\kappa$ B and MX1. RT-qPCR was performed with Applied Biosystems Assays-on-Demand probe and primer combinations and universal reaction mixture, in an ABI 7500 Fast Real-Time PCR System (Applied Biosystems). The  $\beta$ -glucuronidase complex (*GUS*) gene was used for normalization. Results are expressed according to the  $\Delta\Delta C_T$  method, as described by the manufacturer.

**TLR3 agonists and viral stimulation.** We used a synthetic analogue of dsRNA, (polyinosinic:polycytidylic acid (poly(I:C)); Amersham), a TLR3 agonist, at a concentration of 25  $\mu\text{g ml}^{-1}$ . After incubation with or without poly(I:C) for 2, 4 or 6 h, cells were collected in Trizol for RNA extraction. For HSV-1 infection, we used the KOS-1 strain, at a multiplicity of infection (MOI) of 1. A GFP-expressing HSV-1 (HSV-1-GFP<sup>28</sup>) was used at various MOIs to infect NSCs, neurons, oligodendrocytes and astrocytes.

**Cytokine determinations.** The production of IFN- $\alpha$ , IFN- $\beta$ , IFN- $\lambda$  and IL-6 was assessed by enzyme-linked immunosorbent assay (ELISA). Separate ELISAs were carried out for each of IFN- $\alpha$  (AbCys SA), IFN- $\beta$  (TFB, Fujirebio) and IL-6 (Sanquin), according to the kit manufacturers' instructions. The IFN- $\lambda$  ELISA was developed in the laboratory, as described previously<sup>42</sup>.

**HSV-1-GFP infection and quantification.** For HSV-1-GFP infection, 10<sup>4</sup> NSCs, neurons, oligodendrocytes or astrocytes were plated in individual wells of 96-well plates and infected with HSV-1-GFP, at various MOI, in a medium appropriate for the cell type concerned. Cells were incubated for 2 h, then washed and incubated in 100  $\mu\text{l}$  of culture medium. HSV-1-GFP titres were determined by measuring the GFP fluorescence density. The GFP fluorescence of the samples was quantified at the 2, 8, 18 and 24 h after the start of experimentation. For assays of cell protection after viral stimulation, cells were treated with IFN- $\alpha$ 2B (10<sup>4</sup> international units (IU) ml<sup>-1</sup>; Schering-Plough), IFN- $\beta$  (10<sup>4</sup> IU ml<sup>-1</sup>; PBI Interferonsource), IFN- $\lambda$ 1 (2.5  $\mu\text{g ml}^{-1}$ ; R&D Systems), poly(I:C) (25  $\mu\text{g ml}^{-1}$ ), CpG-A (5  $\mu\text{g ml}^{-1}$ ; Dynavax Technologies) or CpG-C (5  $\mu\text{g ml}^{-1}$ , Dynavax

Technologies) for 36 h before infection for neurons, oligodendrocytes, NSCs and astrocytes, as appropriate.

**Statistical tests.** Mean values of IFN induction levels or HSV-1-GFP levels, from control cells and patients' cells, were compared using ANOVA and/or Student's *t*-tests, as implemented in the procedures PROC TTEST and PROC ANOVA of SAS version 9.1 (SAS institute). ANOVA was carried out to compare the means of more than two groups. When significant ( $P < 0.05$ ), ANOVA was followed by *t* tests for pairwise comparisons (in particular, Dunnett's *t* tests comparing the patient with each of the controls).

31. Park, I. H. *et al.* Disease-specific induced pluripotent stem cells. *Cell* **134**, 877–886 (2008).
32. Barberi, T. *et al.* Neural subtype specification of fertilization and nuclear transfer embryonic stem cells and application in parkinsonian mice. *Nature Biotechnol.* **21**, 1200–1207 (2003).
33. Perrier, A. L. *et al.* Derivation of midbrain dopamine neurons from human embryonic stem cells. *Proc. Natl Acad. Sci. USA* **101**, 12543–12548 (2004).
34. Somers, A. *et al.* Generation of transgene-free lung-disease specific human iPSC cells using a single excisable lentiviral stem cell cassette. *Stem Cells* **28**, 1728–1740 (2010).
35. Mostoslavsky, G., Fabian, A. J., Rooney, S., Alt, F. W. & Mulligan, R. C. Complete correction of murine Artemis immunodeficiency by lentiviral vector-mediated gene transfer. *Proc. Natl Acad. Sci. USA* **103**, 16406–16411 (2006).
36. Li, H. & Durbin, R. Fast and accurate short read alignment with Burrows-Wheeler transform. *Bioinformatics* **25**, 1754–1760 (2009).
37. McKenna, A. *et al.* The Genome Analysis Toolkit: a MapReduce framework for analyzing next-generation DNA sequencing data. *Genome Res.* **20**, 1297–1303 (2010).
38. Li, H. *et al.* The Sequence Alignment/Map format and SAMtools. *Bioinformatics* **25**, 2078–2079 (2009).
39. Ying, S. W. & Goldstein, P. A. Propofol-block of SK channels in reticular thalamic neurons enhances GABAergic inhibition in relay neurons. *J. Neurophysiol.* **93**, 1935–1948 (2005).
40. Ying, S. W. *et al.* Dendritic HCN2 channels constrain glutamate-driven excitability in reticular thalamic neurons. *J. Neurosci.* **27**, 8719–8732 (2007).
41. Park, I. H. *et al.* Reprogramming of human somatic cells to pluripotency with defined factors. *Nature* **451**, 141–146 (2008).
42. Yang, K. *et al.* Human TLR-7-, -8-, and -9-mediated induction of IFN- $\alpha$ / $\beta$  and - $\lambda$  is IRAK-4 dependent and redundant and redundant for protective immunity to viruses. *Immunity* **23**, 465–478 (2005).